Earthquakes and Structures, *Vol. 15, No. 6 (2018) 639-654*
DOI: https://doi.org/10.12989/eas.2018.15.6.639

Mushroom skeleton to create rocking motion in low-rise steel buildings to improve their seismic performance

Vahid Mahdavi[1a], Mahmood Hosseini[*2] and Alireza Gharighoran[3b]

[1]*Department of Civil Engineering, Isfahan (Khorasgan) Branch, Islamic Azad University, Isfahan, Iran*
[2]*Structural Engineering Research Center, International Institute of Earthquake Engineering and Seismology (IIEES),Tehran, Iran*
[3]*Faculty of Civil and Transportation Engineering, University of Isfahan, Isfahan, Iran*

(Received August 2, 2018, Revised October 10, 2018, Accepted October 26, 2018)

Abstract. Rocking motion have been used for achieving the 'resilient buildings' against earthquakes in recent studies. Low-rise buildings, unlike the tall ones, because of their small aspect ratio tend to slide rather than move in rocking mode. However, since rocking is more effective in seismic response reduction than sliding, it is desired to create rocking motion in low-rise buildings too. One way for this purpose is making the building's structure rock on its internal bay(s) by reducing the number of bays at the lower part of the building's skeleton, giving it a mushroom form. In this study 'mushroom skeleton' has been used for creating multi-story rocking regular steel buildings with square plan to rock on its one-by-one bay central lowest story. To show if this idea is effective, a set of mushroom buildings have been considered, and their seismic responses have been compared with those of their conventional counterparts, designed based on a conventional code. Also, a set of similar buildings with skeleton stronger than code requirement, to have immediate occupancy (IO) performance level, have been considered for comparison. Seismic responses, obtained by nonlinear time history analyses, using scaled three-dimensional accelerograms of selected earthquakes, show that by using appropriate 'mushroom skeleton' the seismic performance of buildings is upgraded to mostly IO level, while all of the conventional buildings experience collapse prevention (CP) level or beyond. The strong-skeleton buildings mostly present IO performance level as well, however, their base shear and absolute acceleration responses are much higher than the mushroom buildings.

Keywords: resilient building; directed-damage design; mushroom skeleton; energy dissipators; seismic performance level; nonlinear time history analyses

1. Introduction

Most of current seismic design codes accept heavy damages to the buildings in case of major earthquakes, provided that they are prevented against collapse, however, if a building is designed in such a way, most probably it will not be usable after the earthquake and will not fulfill the requirements of the immediate occupancy (IO) performance level (PL). In case of large populated cities, this lack of performance leads to several unacceptable consequences, including: 1) the necessity of evacuating and providing thousands, even hundreds of thousands of people, who have lost their living or working place, with appropriate place(s) for living and/or working; 2) the need to demolishing severely damaged (but not collapsed) buildings, which is a very difficult task, because of the considered ductility, according to seismic design provisions, which lead to creation of a large number of plastic hinges in beams and columns, causing large deformation of the building without complete failure; 3) the necessity of removing the debris of the demolished buildings, which may weigh over millions of tons; and requires thousands of trucks and a very large suitable place for disposal, and 4) plenty of time and cost as well as enormous skillful human forces needed for the reconstruction works of the new buildings to replace the demolished ones (Hosseini *et al.* 2013). The case of Christchurch earthquake of 11 March 2011, in which hundreds of buildings had to be demolished due to heavy damages, can be mentioned as an example case of these unacceptable consequences (Kam *et al.* 2011).

Considering the above facts, in recent years, development of earthquake resistant systems, in which the main members of the structure are prevented against damage, has drawn more attention. Seismic isolation and control are among the techniques proposed in this regard, however, these two techniques have not been much acknowledged worldwide because of their costs and the high technology required for their implementation. Another way for achieving the abovementioned goal (creation of resilient buildings) is using the Directed-Damage Design (DDD) idea (Hosseini and Ebrahimi 2015). DDD idea is the modified version of Deliberate Direction of Damage idea (Hosseini and Alyasin 1996) and means guiding or directing the damage to some pre-decided parts of the structural system, acting as fuses, so that other parts, namely the main structural system, do not experience any major plastic

∗Corresponding author, Professor
E-mail: hosseini@iiees.ac.ir
[a]Ph.D.Student
E-mail: vahid.mahdavi@ymail.com
[b]Professor
E-mail: gharighoran@yahoo.com

ISSN: 2092-7614 (Print), 2092-7622 (Online)

deformation, and therefore making the building structure easily repairable, even after major earthquakes.

One technique for implementing the DDD idea, and achieving resilient buildings, is damage localization by employing energy dissipators and creation of rocking motion capability in the building's structural system. In such a system, relative motion occurs mainly between the bottom of columns and their corresponding foundation where energy dissipators are placed, and the building's structure moves almost as a rigid body. In this way the system is given a kind of smartness. It is worth mentioning that, typically, smart systems are defined as structural systems with a certain-level of autonomy relying on the embedded functions of sensors, actuators and processors that can automatically adjust structural characteristics, in response to the change in external disturbances and environments, toward structural safety and serviceability as well as the elongation of structural service life (Otani *et al.* 2000). This is while the rocking system has neither specific electronic parts nor computer control system(s), but satisfies this definition, and hence, it has been thought that the rocking system is one of the simplest smart structural systems (Azuhata*et al.* 2002, Midorikawa*et al.* 2006).

It should be notedthat since early 70sthe use of rocking motion as a useful way for employing more efficient energy dissipation devices (Kelly *et al.* 1972) and mechanisms (Priestley 1978) for seismic response reduction of structures has been taken into consideration. Since then, rocking columns (Nakahara and Nagase 2000), rocking walls (Ma *et al.* 2005, Khanmohammadi and Heydari 2015, Pollino 2015, Nicknam and Filiatrault 2015), rocking core (Nielsen *et al.* 2010, Qu *et al.* 2014), and rocking frames (Azuhata *et al.* 2002, Midorikawa *et al.* 2006, Eatherton *et al.* 2014, Kafaeikivi *et al.* 2016) have been paid attention and studied for seismic response reduction purpose. However, using the rocking motion for the whole building, in which the building moves almost as a rigid body, as a seismic response reduction technique has been taken into consideration just recently (Hosseini and Ebrahimi 2015).

As Hosseini and Ebrahimi (2015) describe, creation of rocking motion capability in the whole building's structure as a seismic response reduction technique, is taken place : 1) allowing the lowest story columns of the building to uplift, 2) considering a relatively stiff structural system, 3) using a grid-of-stiff-girders at base level, and 4) employing specific energy dissipators, working during the relative motion of bottom of columns at the lowest story with respect to their foundation. It is worth mentioning that another advantage of rocking structural system is its recentering capability. In fact because of the building's weight the structure returns back to its initial position after the earthquake. Nevertheless, it should be noted that this rocking mechanism is not applicable to buildings with aspect ratio smaller than 2, namely mid-rise and low-rise buildings. In fact, low-rise buildings tend to move in sliding mode (if not fixed to the ground) rather than rocking mode. On this basis, some techniques similar to rocking have been proposed for these buildings. Hosseini and Noroozinejad Farshangi (2012), Hosseini and colleagues (2013), Hosseini and Alavi (2014), Hosseini and colleagues (2016), Nejati and Hosseini (2017) have proposed structural systems with capability of seesaw motion. Also, Hosseini and Bozorgzadeh (2013) and Khalkhali and colleagues (2017) have suggested partitioning the building skeleton into four dynamically interactive parts, so that each part can do rocking motion independently.

As an alternative technique, in this study the use of mushroom-form skeleton is proposed for creation of rocking motion in low-rise buildings. In this technique, with a series of orthogonal beams, in the first story of the building, the weight of the building is transferred to a few interior columns, which are allowed to uplift to give the building's structure the capability of rocking motion. At the lower part of each of these columns an energy dissipating device can be used. In this research yielding plate dampers have been considered for this purpose. To illustrate the performance of the proposed system several mushroom-shape rocking buildings, with 3 to 7 stories were considered and their seismic responses were evaluated by a series of nonlinear time history analyses (NLTHA), and compared with those of their conventional counterpart conventional buildings, designed based on a common seismic design code, and also with responses of buildings strengthened by using stronger structural elements, including columns, beams and bracings, called strong-skeleton buildings, to achieve the IO performance level. The response values considered for comparison include maximum inter-story drift, maximum roof acceleration and maximum roof displacement, maximum base shears, and finally plastic hinges formed in the skeleton. In the following sections, first the features of the proposed mushroom skeleton for creation of rocking motion in low-rise buildings is explained. Then, the buildings considered for the study, including mushroom rocking buildings and their conventional counterpart buildings, as well as the strong-skeleton buildings are introduced. In the next step, the earthquakes selected for conducting NLTHA are introduced along with the results of NLTHA, and finally the aforementioned responses are compared, and concluding remarks are presented.

2. The mushroom skeleton for creating low-rise rocking buildings

Tall buildings, due to their large aspect ratio, tend to do rocking motion. This is while during an earthquake low-rise buildings, with large horizontal dimensions and small aspect ratio, tend to sliding, if are not fixed to the ground, rather than moving in rocking mode. However, since seismic response reduction is much easier in rocking mode than sliding mode, it is desired to create the capability of rocking motion in these buildings as well. It is worth mentioning that rocking structural system can be considered as a passive smart system. A way for achieving this goal is to make the building rock on its internal bay(s) by creating a lower story at the center of the building with only one or two bays in both directions, giving a mushroom form to the building skeleton as shown in Figs. 1 and 2.

As it is seen in Figs. 1-2, there is a grid of strong girders

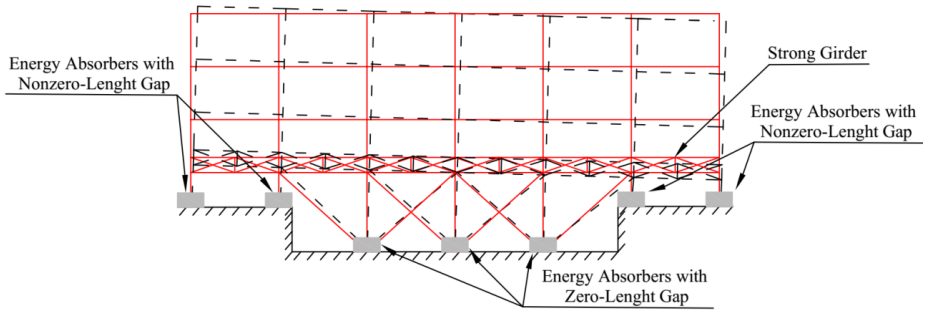

Fig. 1 A middle frame of the 'mushroom skeleton' of a low-rise rocking building, capable of rocking on its two central bays

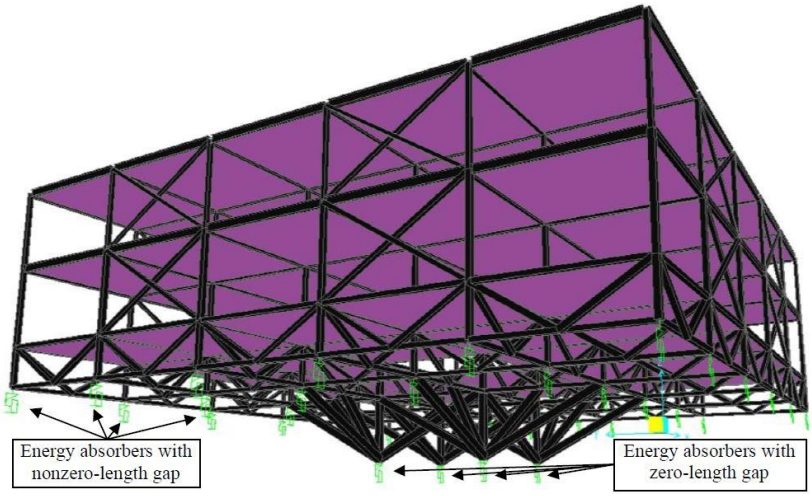

Fig. 2 A looking-from-the-bottom perspective view of the mushroom skeleton of a rocking low-rise building, capable of rocking on its single central bay

(GOSG) at the lowest story of the building's structure resting on a supporting truss of which the columns of the central bay(s) act as the vertical members. The GOSG acts, in fact, as an almost rigid foundation for the upper stories of the buildings and helps the building's structure to remain basically elastic during earthquake excitations, provided that it has sufficiently large stiffness. Between either the supporting truss or GOSG and foundation of the building, there are a set of energy dissipating devices as shown in the figures. It should be noted that there are zero-length gaps between the lower ends of the columns of the central bay(s), on which the building's skeleton rocks, while in case of other supports of the GOSG there are nonzero-length gaps in which the amount of gap is proportional to its horizontal distance from the corresponding column of the central axes of the building's structure, to accommodate the rocking motion of the building. The amounts of initial stiffness and the yielding force of the nonzero-length gaps are obtained based on some basic criteria as explained in section 4 of the paper. Fig. 3 shows the details of the employed energy absorbers of the two types of zero-length and nonzero-length gaps.

The role of energy absorbers, shown in Fig. 3, is dissipating the major part of the earthquake input energy at foundation level, so that the amount of energy inserted into the upper stories, and as a result the seismic damages imposed to the building's main structural members become minimal. In case of columns of the central bays on which the building's skeleton does its rocking motion, energy dissipation takes place when the columns' lower ends move upward above the foundation level and returns back downward. During these upward and downward motions, as shown in Fig. 3, each yielding plate bends first in upward motion and then in downward motion, and dissipates energy by its plastic deformation. This is while, in case of other supports, energy dissipation takes place by plastic bending of yielding plates in both downward motion below their initial level and upward motion above it.

3. Introducing the considered buildings for seismic evaluation

In this study, a set of regular steel residential buildings with 3 to 7 stories with story height of 4.0 meters for the lowest story and 3.0 meters for upper ones, all having square plan with 5 bays in both directions each spanning 5.0 meters, have been considered. Fig. 4 shows the plan, the 3-D view, and the internal and external frames of the 3-story conventional building as a sample of the considered buildings.

The considered buildings were designed first as conventional buildings based on a conventional seismic design code (AISC-ASD, which is still being used in many parts of the world), considering the dual moment frame and X-bracing as their lateral load bearing system. The

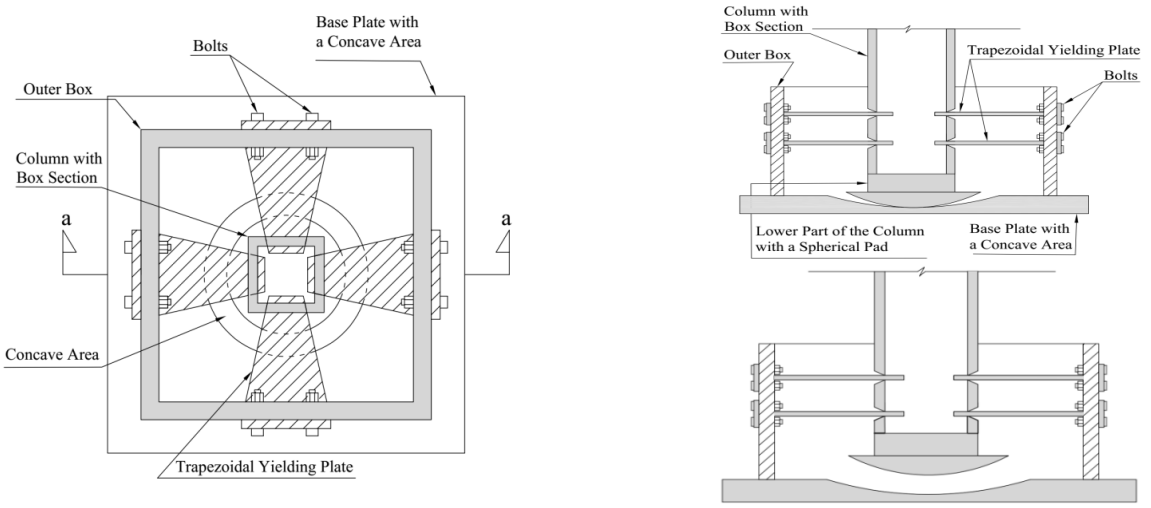

Plan view of the yielding-plate dampers (left) and the section of its zero-length gap type (upper right) and nonzero-length gap type (lower right)

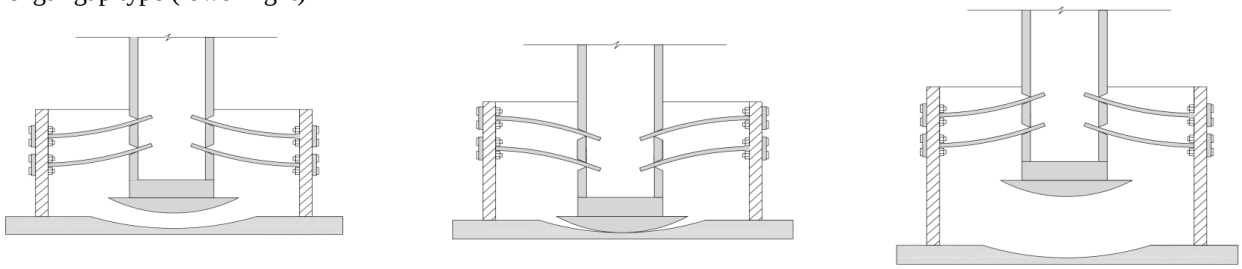

Section of the zero-length gap damper in motion above the initial level of the column's bottom (left), and that of nonzero-length gap damper in motion below the initial level of the column's bottom (middle) and above the initial level of the column's bottom (right)

Fig. 3 Plan view and sections of zero-length and nonzero-length gap yielding-plate dampers

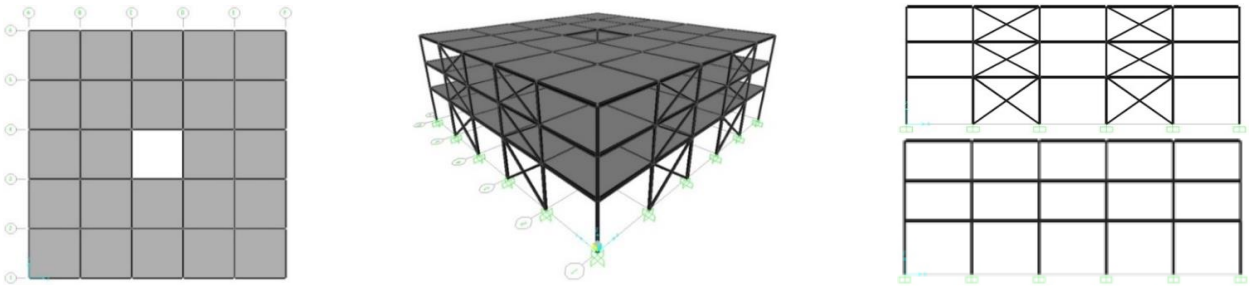

Fig. 4 The plan, a 3-D view and the internal and external frames of the 3-story conventional building

Table 1 Materials properties used for design of the considered buildings

Steel Material Properties					
f_u (kg/m^2)	f_y (kg/m^2)	ϑ	E (kg/m^2)	W (kg/m^3)	M (kg.f/m^3)
3700×10^4	2400×10^4	0.3	2.1×10^{10}	7850	800

materials properties used for design are presented in Table 1.

It was tried to make the amount of overstrength as low as possible in the skeleton of these buildings to have an economic design. The used sections for the structural member are presented in the Appendix. Fig. 5 shows a color representation of demand over capacity ratio (D/C) of the structural elements in case of the 3-story building, and Table 2 presents the natural periods of the three lower modes of the conventional buildings.

It is seen that the first and second modal periods are almost equal, as expected, because of the symmetric skeleton of the buildings. The slight difference between these values is due to the effect of stair landing beams at the mid-height of columns of the staircase, which exist only in one direction, and slightly increase the stiffness of skeleton in one direction comparing to the other. In the next step, the conventional buildings' skeletons were changed to rocking structure by using mushroom form structures, as described in section 2. In the computer model of mushroom buildings the energy absorbers were introduced by multi-linear plastic springs in combination with nonzero- and/or zero-length gap elements, depending on the situations of the columns. The appropriate values for initial stiffness and yielding strength of multi-linear plastic springs as well as the stiffness of gap elements were found by a series of trial and

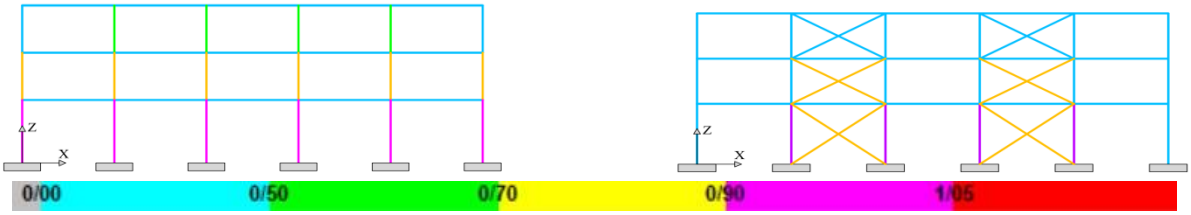

Fig. 5 Color representation of D/C values for the main structural elements in case of the 3-story conventional building

Table 2 The natural periods (in sec) of the six lower modes of the conventional buildings

Number of Stories	Mode Number					
	1 (Lateral)	2 (Lateral)	3 (Torsional)	4 (Lateral)	5 (Lateral)	6 (Torsional)
3	0.474	0.473	0.295	0.145	0.145	0.106
4	0.579	0.577	0.359	0.184	0.183	0.114
5	0.694	0.693	0.433	0.224	0.224	0.141
6	0.830	0.829	0.520	0.252	0.252	0.159
7	0.958	0.956	0.614	0.292	0.29	0.187

error process through conducting several cases of NLTHA on 2-D models of the mushroom building, meeting the drift ratio code provisions, and achieving the desired performance level (LS or higher) based on formation of plastic hinges (PHs) as described in the main report of the study (Mahdavi 2018).

It should be noted that, in addition to the basic changes in the buildings' skeletons, as described in the previous section, to keep the seismic performance level of rocking buildings at the desired IO level, it was necessary to replace a few of the structural members with stronger ones. For example, in case of 3-story building the columns of the braced bays in the second story of the external frames were of Box 150×10 profile in case of conventional building, while they had to be replaced by Box 180×15 in case of rocking building. For taller buildings the amount of this upgrade was a little more. It is obvious that these replacements slightly increase the skeleton's weight of the rocking buildings, in addition to the extra weight of GOSG and supporting truss as the substructure of the mushroom skeleton. Replacement of a few structural members of the mushroom buildings for providing the desired high performance level of IO, may raise this question in mind that how much members' upgrading (without any changes in the configuration of the skeleton) can improve the conventional buildings' seismic performance level from CP or a lower level to LS or a higher level. On this basis, it was decided to substitute some elements of the skeleton of conventional buildings by stronger elements to upgrade the building's seismic performance mostly to IO level, subjected to the employed earthquakes. This process was also based on trial and error and was done by repeated NLTHA (Mahdavi 2018 [19]). The selected earthquakes for conducting the required NLTHA and the obtained results are presented in the next section.

4. NLTHA of the considered buildings

Table 3 Specification of seven selected earthquake for NLTHA

Earthquake	PGA Values in Main Direction (g)			1st Dominant Period (s)	2nd Dominant Period (s)	Effective Duration (s)
	X	Y	Z			
Chi-Chi	0.339	0.398	0.166	0.91	0.17	35
Imperial Valley	0.367	0.379	0.144	0.26	0.18	10
Kobe	0.483	0.464	0.387	0.47	0.22	13
Kocaeli	0.312	0.364	0.206	0.39	0.30	13
Manjil	0.515	0.497	0.538	0.16	0.34	31
Northridge	0.443	0.488	0.325	0.53	0.87	10
Superstition Hills	0.357	0.259	0.128	0.19	0.45	38

For seismic evaluation of the considered buildings by conducting a series of NLTHA and finding out the efficiency of the proposed mushroom shape rocking structures in seismic response reduction of buildings, the three-component accelerograms of seven far-field earthquakes were selected based on FEMA P695 (2009) guidelines, so that their dominant periods fall between 0.4 and 1.0 second (the period range of the considered conventional buildings in lateral modes according to Table 1). Table 3 presents the specifications of selected earthquakes, and Fig. 6 shows the SRSS acceleration spectra of their two horizontal components.

Scaling of the records for NLTHA was done based on ASCE 41-13 (2013) guidelines. For this purpose, a square root of the sum of the squares (SRSS) spectrum was constructed for each pair of horizontal ground motion acceleration histories, by taking the SRSS of the 5% damped response spectra for the scaled components with an identical scale factor applied to both components of a pair. Scaling for each pair was performed such that in the period range from 0.2T to 1.5T (T being the fundamental period of the building) the average of the SRSS spectra from all horizontal acceleration history pairs did not fall below the corresponding ordinate of the target response spectrum, which was in this study the ASCE 7-16 spectrum for soil type C. This spectrum is very similar to the spectrum given in Iranian Standard No. 2800 for soil type II, considered for the site of the buildings in this study. Table 4 presents the scale factors obtained by the explained method for all of the selected earthquakes.

For modeling the nonlinear behavior of the structural elements, the FEMA curves were used for beams, columns and bracing elements, a bilinear model shown in Fig. 7 was used for the yielding-plate energy absorbers, and a general

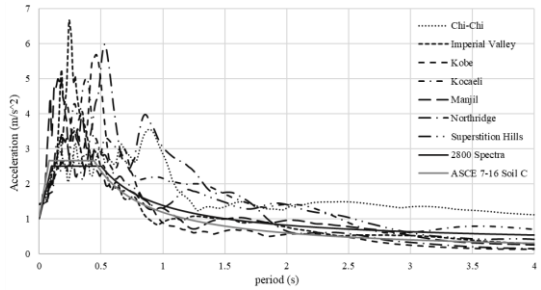

Fig. 6 SRSS acceleration spectra of the selected earthquakes

Table 4 Scaled PGA values of the selected records obtained by the ASCE 41-13 guideline method for scaling the accelerograms

Earthquake	Number of Stories				
	3	4	5	6	7
Chi-Chi	4.15	4.15	4.15	4.10	4.10
Imperial Valley	4.36	4.12	4.12	4.80	5.80
Kobe	4.46	4.30	4.30	4.00	4.50
Kocaeli	4.84	4.80	4.80	4.80	4.80
Manjil	3.88	4.12	4.12	4.12	4.12
Northridge	4.30	4.20	4.20	4.20	4.20
Superstition Hills	4.25	4.25	4.25	4.00	4.00

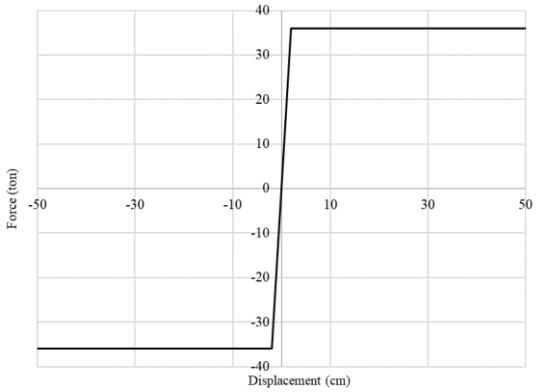

Fig. 7 The bilinear model used for the yielding-plate energy absorbers

damping of 5% was also assumed for all of the considered structural models.

The responses considered for seismic evaluation of the three groups of the considered buildings and their comparison, include roof acceleration and roof

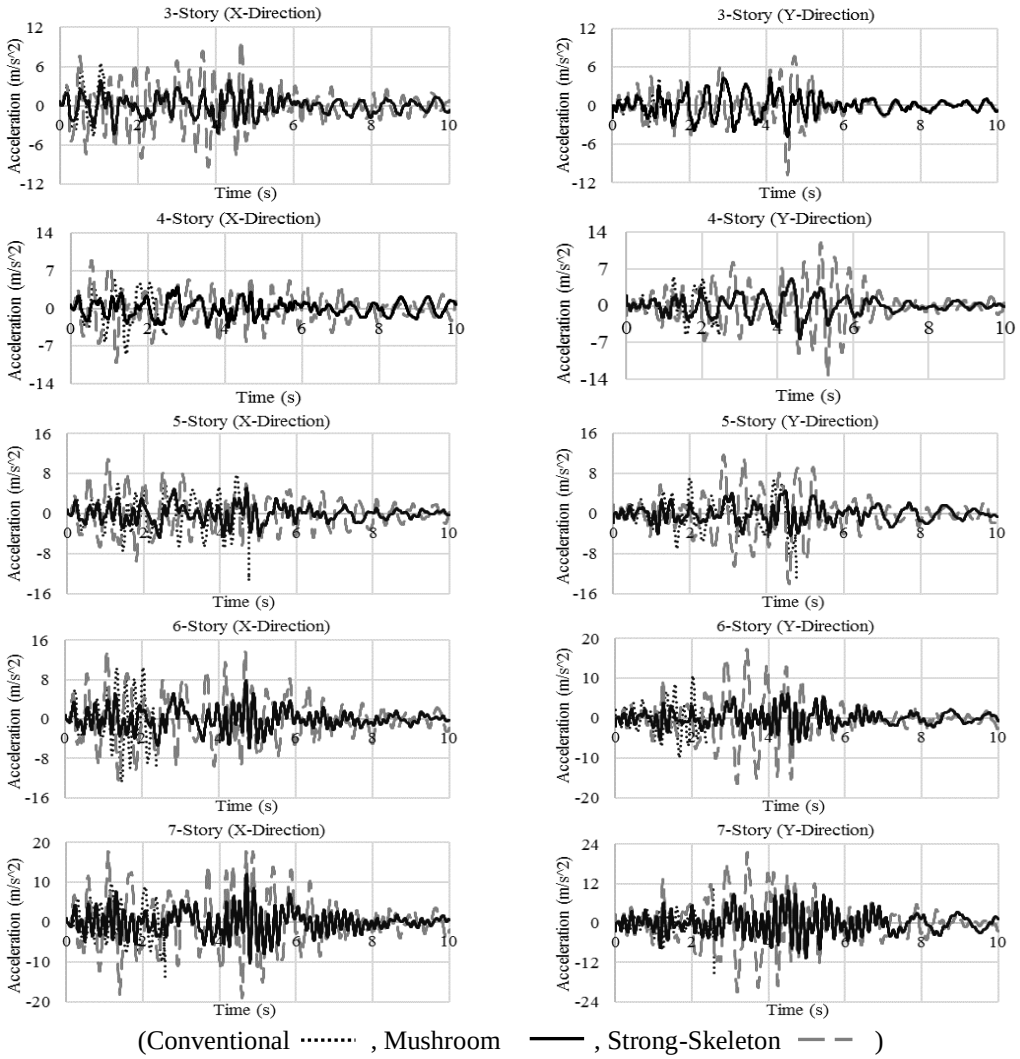

(Conventional ····· , Mushroom ——— , Strong-Skeleton — —)

Fig. 8 Comparison of roof acceleration time histories of the considered buildings with conventional strong-skeleton and mushroom skeleton to Imperial Valley earthquake

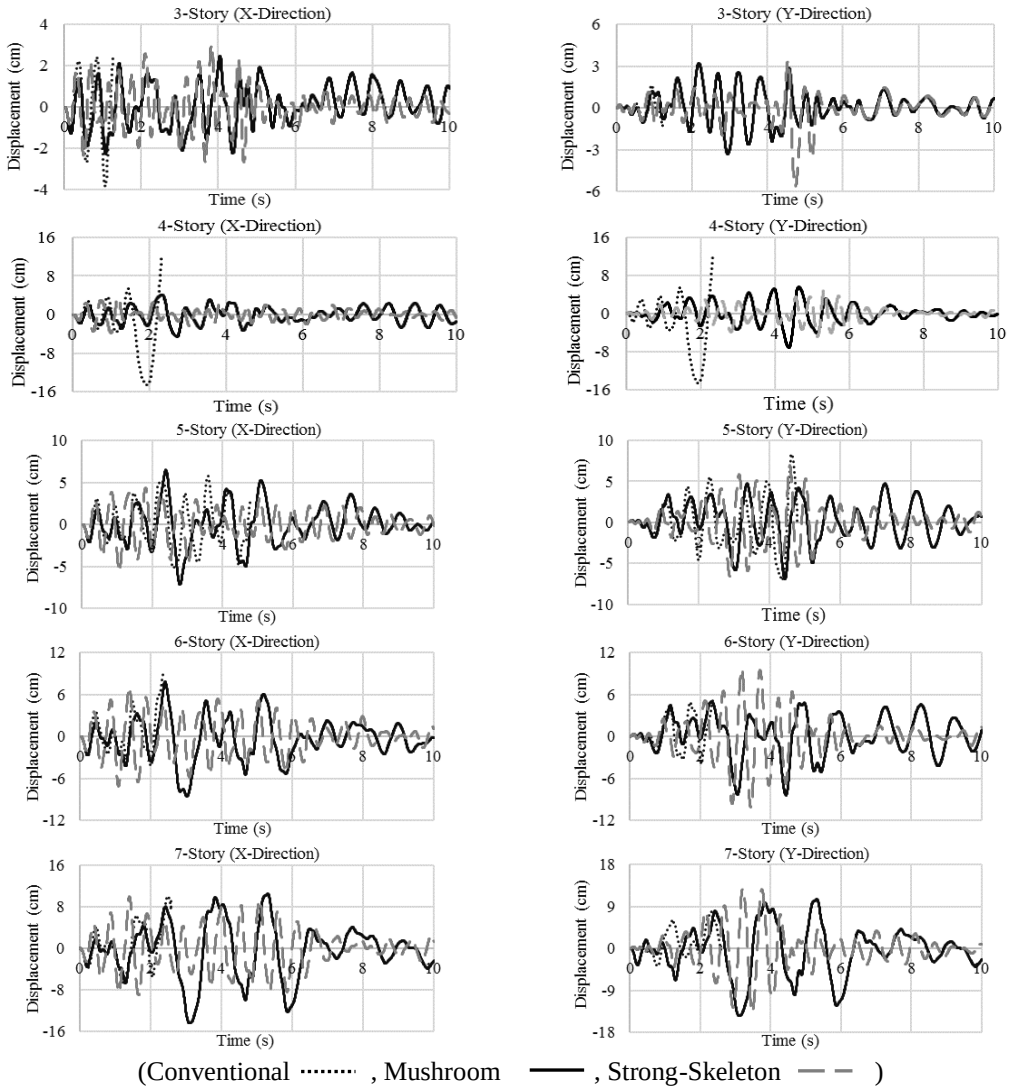

Fig. 9 Comparison of roof displacement time histories of the considered buildings with conventional, strong-skeleton and mushroom skeleton to Imperial Valley earthquake

displacement, base shear, inter-story drifts and formation of PHs. Figs. 8-10 show, respectively, the roof acceleration, roof displacement and base shear time histories of all three groups of buildings in both *X* and *Y* directions, subjected to Imperial Valley earthquake as a sample of the employed earthquakes. It is seen in Figs. 8-10 that conventional buildings all have failed subjected to the scaled records of Imperial Valley earthquake, while the mushroom and strong-skeleton buildings have tolerated the earthquake up to its end. Figs. 8-10 also show that the roof acceleration and base shear responses in case of mushroom buildings are drastically lower than two other groups. This can be basically because of longer period of mushroom buildings on the one hand, and high stiffness of strong-skeleton buildings on the other. Also, it can be seen in Fig. 9 that the maximum roof displacement response in case of mushroom buildings is almost equal to that of strong-skeleton buildings, and in some cases a little larger. However, in all cases it is less than the code recommended value of 0.01 of the building's height (Iranian Standard No. 2800 for seismic design of structures). These results are true in case of other employed earthquakes, however, due to lack of space results related to other earthquakes are not presented here, and can be found in the main report of the study (Mahdavi 2018). To better evaluate the seismic responses of the considered buildings, the inter-story drift values were also obtained from NLTHA. Figs. 11-15 show the maximum drift ratios for all studied buildings in both *X* and *Y* directions, subjected to all seven employed earthquakes.

It is seen in Figs. 11-15 that in most cases the drift values of the conventional buildings have exceeded the code limit, while in the strong-skeleton building they are mostly lower than that limit, as expected. Only in a few cases, which were explained before, the drift values of strong-skeleton buildings have exceeded the code limit. In case of mushroom buildings the drift values are mostly at the code limit or below it. Only in two cases, one related to the top story of the 4-story mushroom building subjected to Chi-Chi earthquake, and the other one related to the top story of the 7-story mushroom building subjected to Imperial Valley earthquake, the drift values have exceeded the code limits. The reason behind these facts, with regard

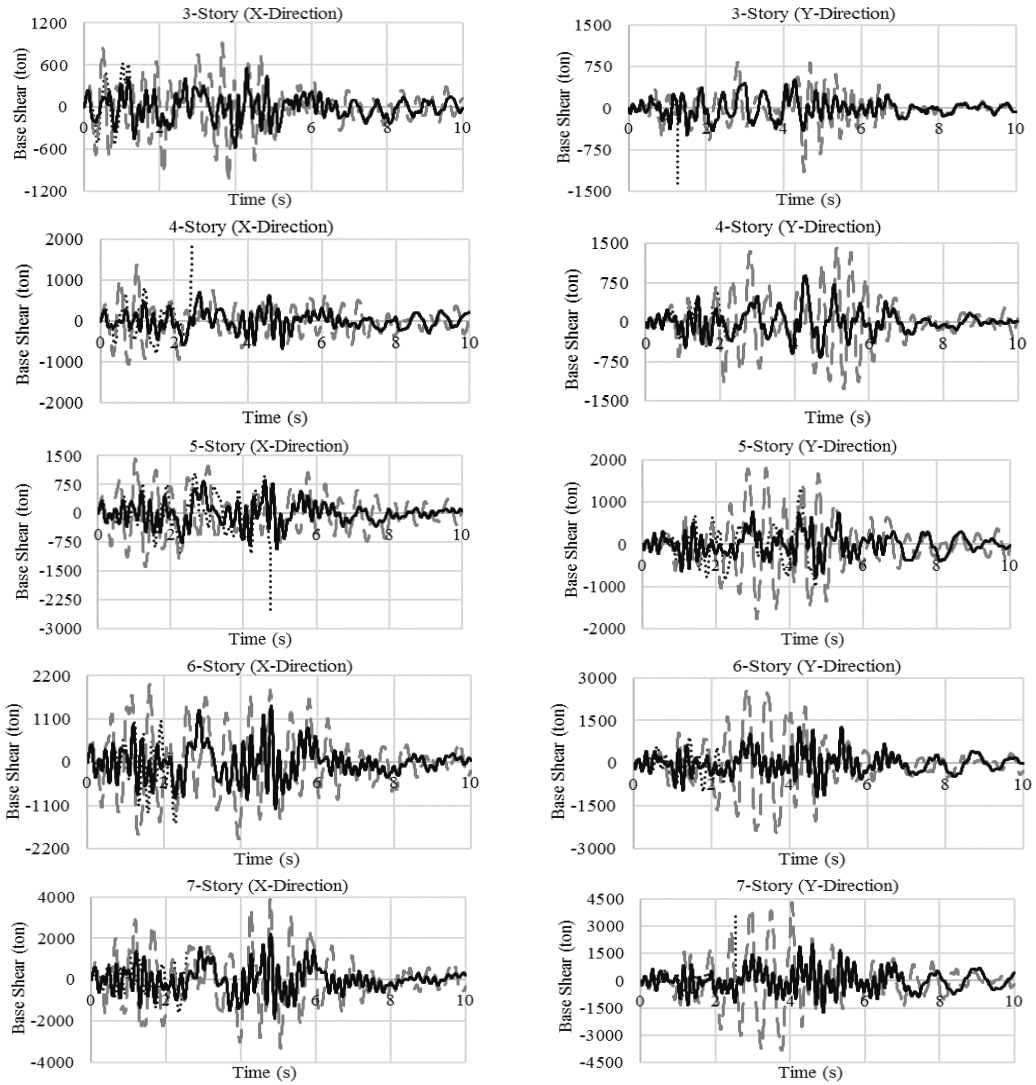

Fig. 10 Comparison of base shear time histories of the considered buildings with conventional, Strong-Skeleton and mushroom skeleton subjected to Imperial Valley earthquake

to the 4-story mushroom building is the existence of a peak in the spectral acceleration of Chi-Chi earthquake close to 0.7 sec, which is the fundamental period of the 4-story mushroom building. With regard to the 7-story mushroom building it can be said that by noticing the pseudo velocity spectrum of Imperial Valley record, shown in Fig. 16, the high energy of this earthquake in the whole period range beyond 0.15 sec. can be realized, which means that this record can excite the higher modes of mushroom buildings as well, particularly its second mode in which excessive motion of the roof occurs, resulting in large drift values at the upper story of the building.

To show the drift ratio results in brief, Table 5 presents the maximum drift ratio values for all mushroom and strong-skeleton buildings subjected to the seven employed earthquakes.

As the last set of NLTHA results, Figs. 17-20 show the PHs formed in some samples frames of the mushroom and strong-skeleton buildings' structures, which have shown various performance levels subjected to different

Table 5 Drift ratios for all mushroom and strong-skeleton buildings subjected to the seven employed earthquakes

No. of Stories	Skeleton Type	Earthquake						
		Chi-Chi	Imperial Valley	Kobe	Kocaeli	Manjil	Northridge	Superstition Hills
3	Mushroom	0.0055	0.0038	0.0047	0.0054	0.0031	0.0061	0.0045
	Strong-Skeleton	0.0032	0.0051	0.0033	0.0093	0.0031	0.0032	0.0023
4	Mushroom	0.0082	0.0067	0.0069	0.0082	0.0059	0.0076	0.0070
	Strong-Skeleton	0.0033	0.0053	0.0052	0.0053	0.0035	0.0047	0.0036
5	Mushroom	0.0112	0.0041	0.0057	0.0088	0.0057	0.0105	0.0086
	Strong-Skeleton	0.0056	0.0033	0.0115	0.0055	0.0031	0.007	0.0051
6	Mushroom	0.0102	0.0045	0.0060	0.0093	0.0054	0.0142	0.0073
	Strong-Skeleton	0.0055	0.0052	0.0075	0.0054	0.0046	0.0147	0.0050
7	Mushroom	0.0083	0.0069	0.0035	0.0124	0.0071	0.0109	0.0083
	Strong-Skeleton	0.0043	0.006	0.0074	0.0066	0.0035	0.0102	0.0043

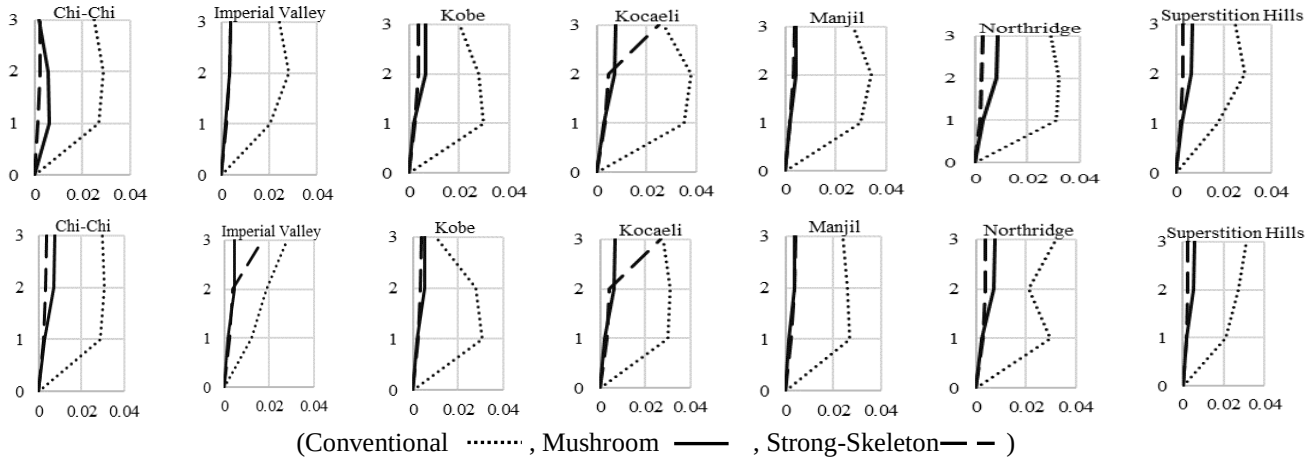

Fig. 11 Maximum inter-story drift ratios of all three groups of the 3-story considered buildings in both *X* (upper figures) and *Y* (lower figures) directions subjected to the seven employed earthquakes

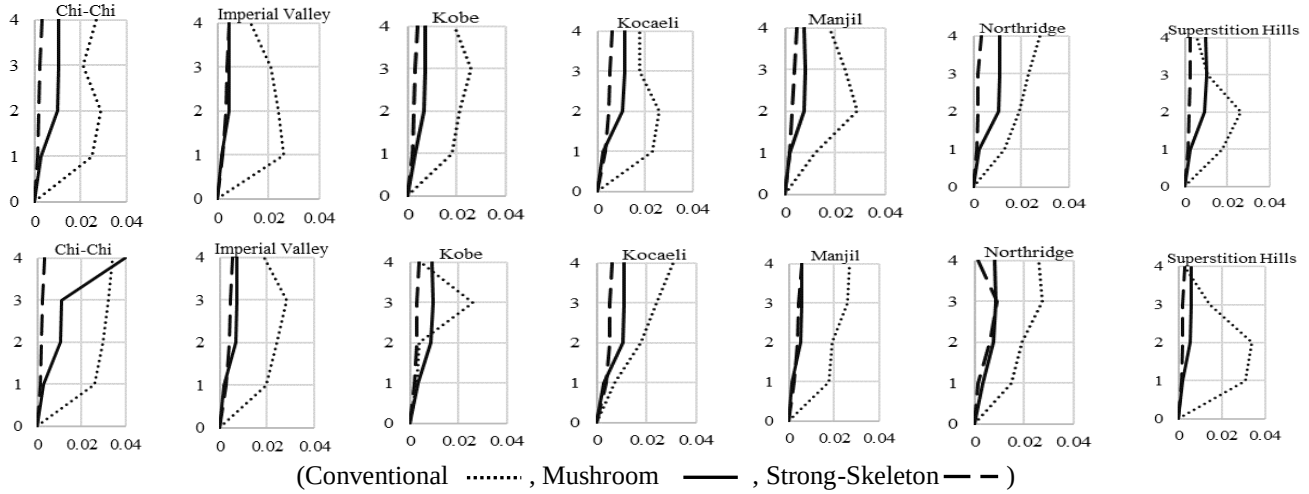

Fig. 12 Maximum inter-story drift ratios of all three groups of the 4-story considered buildings in both *X* (upper figures) and *Y* (lower figures) directions subjected to the seven employed earthquakes

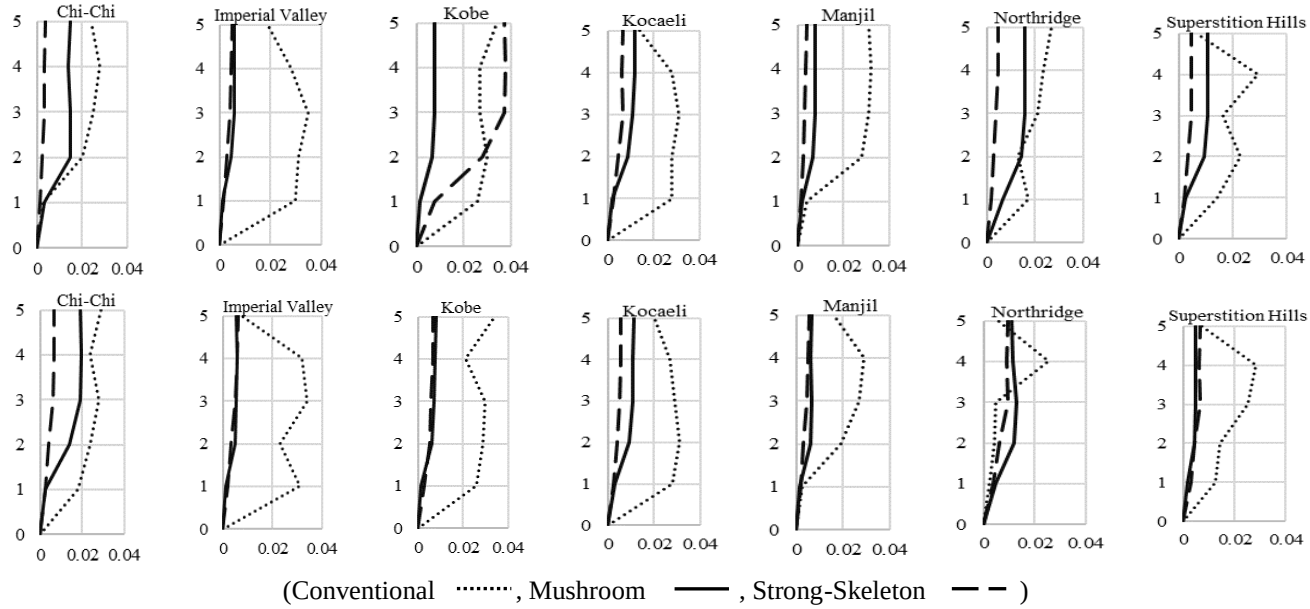

Fig. 13 Maximum inter-story drift ratios of all three groups of the 5-story considered buildings in both *X* (upper figures) and *Y* (lower figures) directions subjected to the seven employed earthquakes

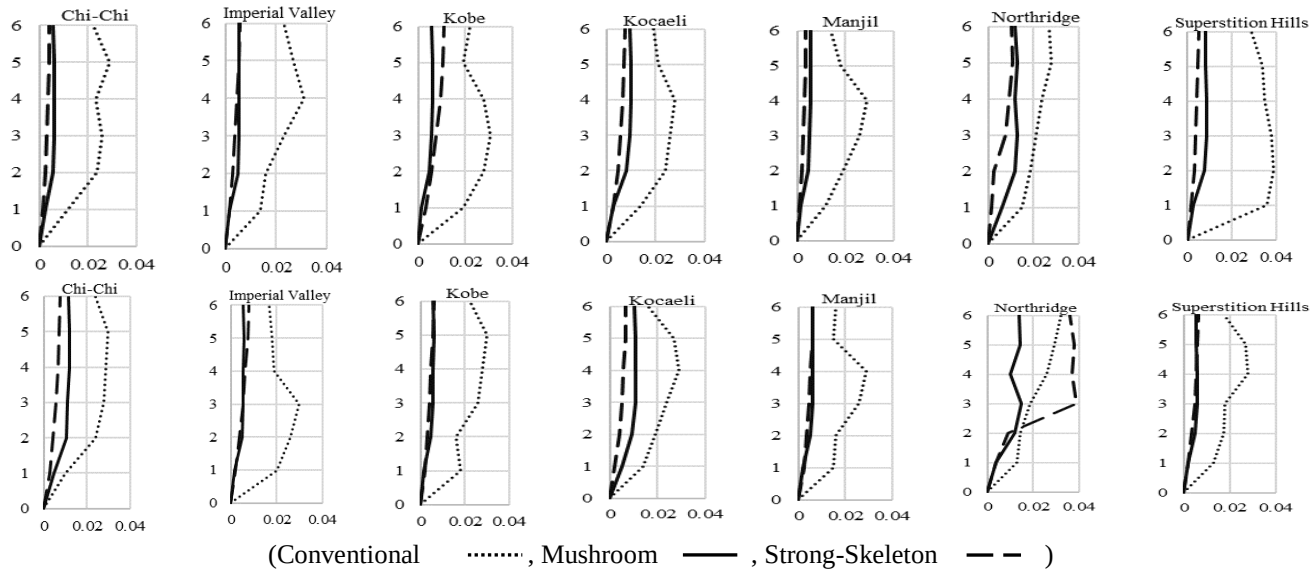

Fig. 14 Maximum inter-story drift ratios of all three groups of the 6-story considered buildings in both *X* (upper figures) and *Y* (lower figures) directions subjected to the seven employed earthquakes

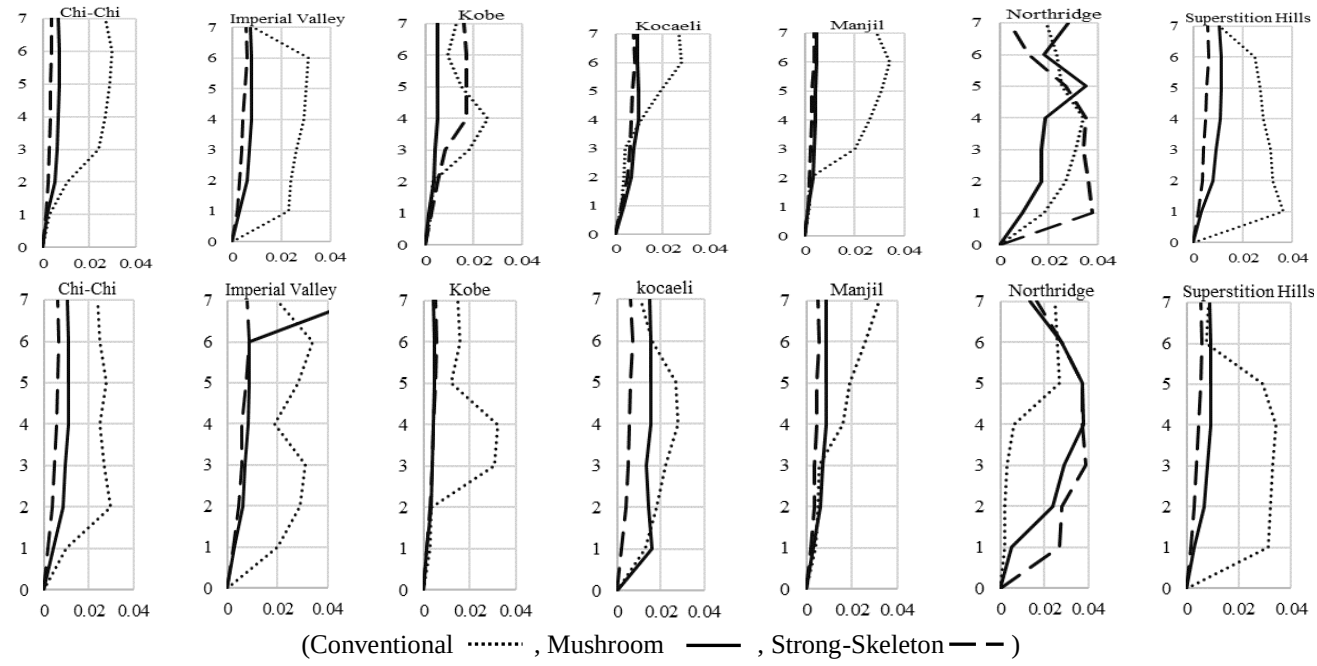

Fig. 15 Maximum inter-story drift ratios of all three groups of the 6-story considered buildings in both *X* (upper figures) and *Y* (lower figures) directions subjected to the seven employed earthquakes

earthquakes.

As it is seen in Fig. 17, most of PHs in mushroom buildings, subjected to Imperial Valley earthquake are at IO level, and very few ones at LS level. The same is true for strong-skeleton building, in which only a few PHs at IO level have formed in its bracing elements, as shown in Fig. 18. Figs. 19-20 show that both mushroom and strong-skeleton 5-story buildings have had an undesirable performance level subjected to Northridge earthquake, with some PHs at collapse level in their bracing elements and also some columns. To have a better general picture of the performance levels of the considered buildings the desirable (LS or higher) and undesirable (CP or lower) performance levels of all considered buildings based on formation of PHs, subjected to all employed earthquakes, are summarized in Table 6.

The reason behind undesirable (Not OK) performance of some mushroom and strong-skeleton buildings against one or two ones of the employed earthquakes, reported in Table 3, can be closeness of their fundamental period values to the dominant periods of those earthquakes, which can be seen in their spectral acceleration curves, shown in Fig. 6, and presented in Table 3. To declare this closeness the fundamental periods of the strong-skeleton and mushroom buildings are presented in Table 7.

It should be noted that in case of mushroom buildings

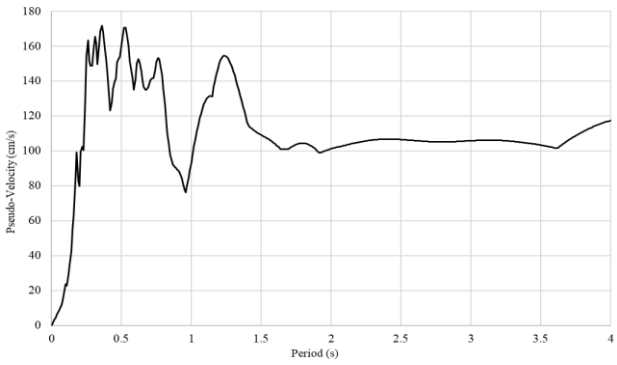

Fig. 16 The pseudo velocity spectrum of Imperial Valley earthquake record

Table 6 Desirable (OK) and undesirable (Not OK) statuses of the considered mushroom and strong-skeleton buildings subjected to the employed earthquakes based on formation of PHs

No. of Stories	Skeleton Type	Earthquake						
		Chi-Chi	Imperial Valley	Kobe	Kocaeli	Manjil	Northridge	Superstition Hills
3	Mushroom	OK	OK	OK	OK	OK	OK	OK
	Strong-Skeleton	OK	OK	OK	OK	OK	OK	OK
4	Mushroom	OK	OK	Not OK	OK	OK	Not OK	OK
	Strong-Skeleton	OK	OK	Not OK	Not OK	OK	OK	OK
5	Mushroom	Not OK	OK	OK	OK	OK	Not OK	OK
	Strong-Skeleton	OK	OK	Not OK	OK	OK	Not OK	OK
6	Mushroom	Not OK	OK	OK	OK	OK	Not OK	OK
	Strong-Skeleton	OK	OK	Not OK	OK	OK	Not OK	OK
7	Mushroom	OK	OK	OK	OK	OK	Not OK	OK
	Strong-Skeleton	OK	OK	Not OK	OK	OK	Not OK	OK

due to the nonlinear behavior of energy absorbers, as well as geometric nonlinearity of rocking motion, theoretically vibration modes cannot be defined, however, at the end of

Table 7 The fundamental periods/pseudo-periods (sec) of the strong-skeleton and mushroom buildings

No. of Stories	Strong-Skeleton Buildings	Mushroom Buildings
3	0.354	0.600
4	0.415	0.700
5	0.477	0.820
6	0.511	0.920
7	0.537	1.060

their seismic response, when the mushroom buildings do some free oscillations, the consequent peak to peak time differences in the response time histories can be considered in average the free vibration period of the system, which be called fundamental pseudo period. Fig. 21 shows two sample time histories of the 7-story mushroom building subjected to Imperial Valley earthquake, in which the free oscillations of the building can clearly be observed.

The seesaw motion of the mushroom buildings can be clearly understood from the oscillations of the two opposite points of the buildings, as shown in Fig. 21. As a sample of the aforementioned closeness it can be seen in Table 4 that the fundamental period of the 5-story strong-skeleton building is 0.477 sec, which is very close to the dominant period of Kobe earthquake, that is 0.45 sec, as given in Table 2. Also it is seen in Table 4 that the pseudo period of the 5-story mushroom building is 0.82 seconds. This value is very close to the second spectral peak in acceleration response spectrum of both Chi-Chi and Northridge earthquakes, and that is why the 5-story mushroom building has not tolerated these two earthquakes without damage. Similar cases have happened for other buildings in which PHs have formed in CP or lower levels. As the last set of NLTHA results, some force–displacement hysteresis curves of the multi-linear plastic springs, used for modeling the nonzero-length gap dampers are presented in Figs. 22 and 23, respectively for two states of non-closure of the gap and its closure.

Looking at Fig. 22, one can realize that the building has done seesaw motion basically with respect to diagonal axis

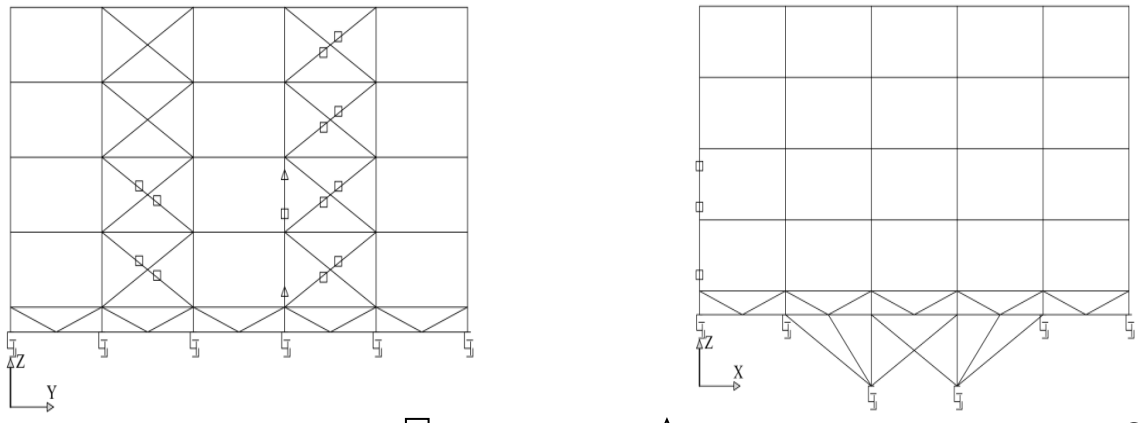

Immediate Occupancy (IO); □ Life Safety (LS); △ Collapse prevention (CP) or beyond it ○

Fig. 17 PHs formed in two sample frames of the 5-story mushroom building with desirable performance levels (LS or higher) subjected to Kocaeli earthquake

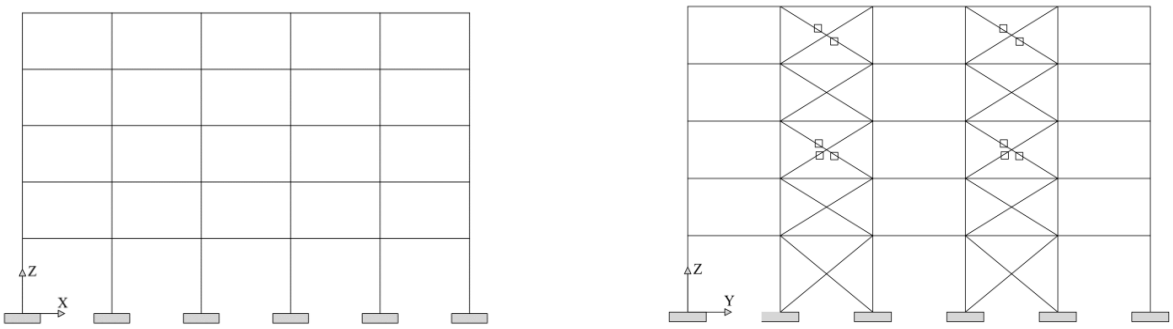

Immediate Occupancy (IO); □ Life Safety (LS); △ Collapse prevention (CP) or beyond it ○

Fig. 18 PHs formed in two sample frames of the 5-story strong-skeleton building with desirable performance levels (LS or higher) subjected to Imperial Valley earthquake

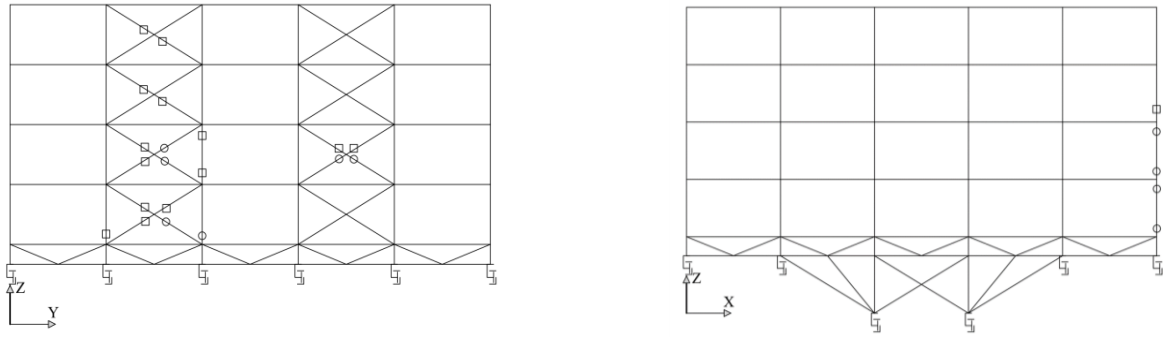

Immediate Occupancy (IO); □ Life Safety (LS); △ Collapse prevention (CP) or beyond it ○

Fig. 19 PHs formed in two sample frames of the 5-story mushroom building with undesirable performance levels (CP or lower) subjected to Northridge earthquake

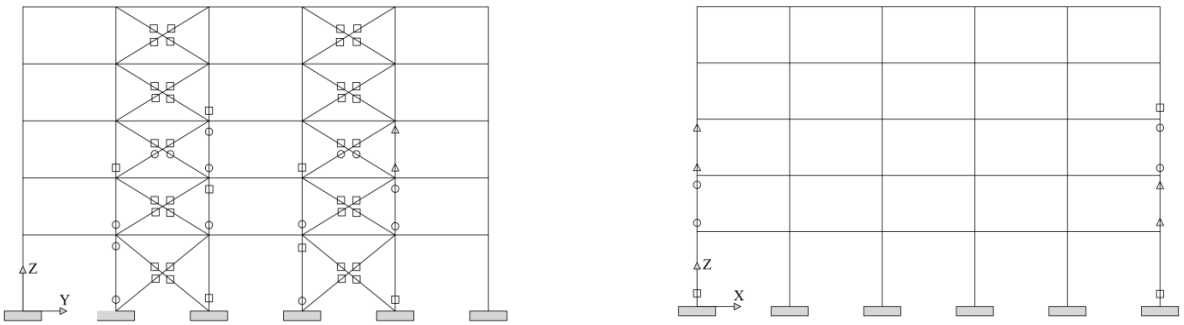

Immediate Occupancy (IO); □ Life Safety (LS); △ Collapse prevention (CP) or beyond it ○

Fig. 20 PHs formed in two sample frames of the 5-story strong-skeleton building with undesirable performance levels (CP or lower) subjected to Northridge earthquake

connecting joints 316 and 351, causing that more vertical deformations take place at links connected to joints 303 and 364. It can be seen in Fig. 21 that at instant of 3.0 seconds displacement value of joint 303 has reached the amount of 10 centimeters (the gap size), which means that the gap closure has occurred, and therefore the stiffness of the GAP element has been activated for a short while of almost 0.2 seconds. This fact can be confirmed by the force-displacement graph of the combination of the multi-linear plastic link and the GAP element, as shown in Fig. 23.

It is seen in Fig. 23 that a maximum force of 318 tons in the GAP element connected to joint 303 of the 7-story mushroom building subjected to Imperial Valley earthquake which is a small value comparing to the axial forces created in the lower corner columns of a 7-story conventional building. To find out how much more steel material is consumed in the mushroom skeleton buildings than strong-skeleton ones, the skeleton weight of all buildings and their ratios are summarized in Table 6 for comparison.

It should be noted that although weights of conventional buildings are much lower than two other groups, the low weight cannot be considered as an advantage, since all conventional buildings have collapsed subjected to all of the applied earthquakes. On this basis, the comparison of weights in Table 8 has done only between mushroom and strong-skeleton buildings.

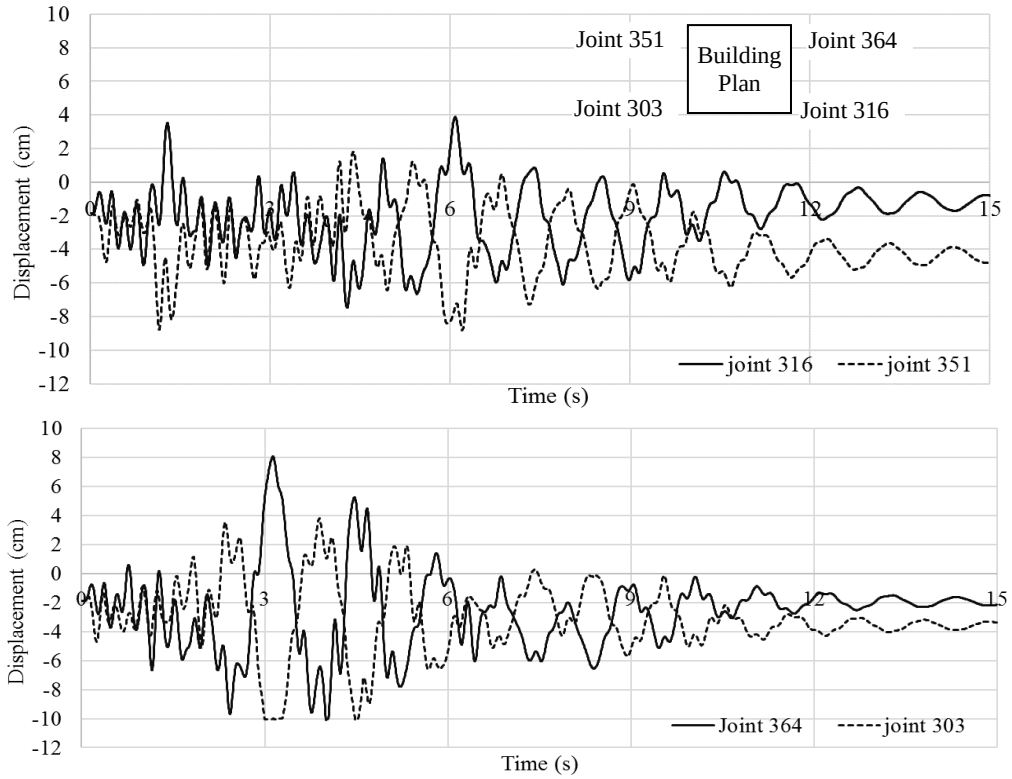

Fig. 21 Two samples of vertical displacement time histories of diagonally opposite nodes at the bottom of GOSGs of the 7-story mushroom building subjected to Imperial Valley earthquake (locations of the joints are shown on the building plan in the upper graph)

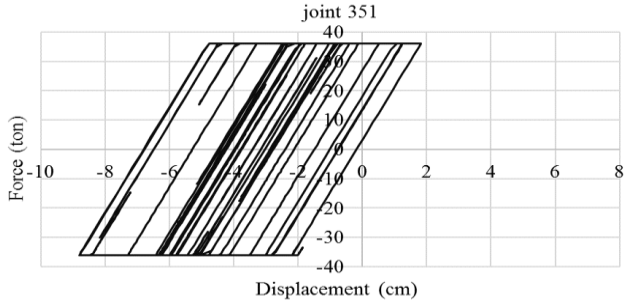

Fig. 22 Force-displacement hysteresis of nonzero-length gap dampers at bottom corner (joint 351 in Fig. 21) of the 7-story mushroom building subjected to Imperial Valley earthquake, in which gap closure has not occurred

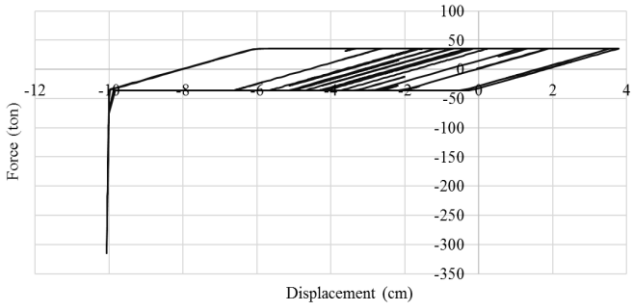

Fig. 23 Force-displacement graph of the combination of the multi-linear plastic link and the GAP element related to joint 303 (see Fig. 19) of the 7-story mushroom building subjected toImperial Valley earthquake, in which gap closure has occurred

Table 8 Buildings' skeleton weights in ton

No. of Stories	Type of Structure			Ratio of Mushroom to Strong-Skeleton
	Conventional	Strong-Skeleton	Mushroom	
3	56.2	79.5	116.17	1.46
4	91.2	122	151.3	1.23
5	123	204	268	1.31
6	173.8	314.3	450.6	1.43
7	188.8	440.2	513.6	1.16

This comparison shows that mushroom skeletons has around 30% more weight than strong-skeletons in average. Regarding that the cost of a building's skeleton is around 30% of the total cost of whole building, the cost of the extra weight will be less than 10% in the total cost of the building.

5. Conclusions

Based on the numerical result of NLTHA conducted on computer models of 3- to 7-story conventional and mushroom building, as well as strong-skeleton buildings, subjected to 7 selected earthquake 3-component accelerograms the following can be made:

- All of the considered conventional buildings collapsed subjected to the employed earthquakes, while the rocking ones showed IO and LS performance levels.

• The strong-skeleton buildings, in spite of their overdesigned structure element could not tolerate some of the applied earthquakes. In cases that these buildings could withstand the earthquake the roof acceleration values have reached up to 2.0 g, while the roof acceleration peak values of the mushroom buildings have been mostly less than half of the peak values of the counterpart strong-skeleton buildings. It is worth mentioning that by making the strong-skeleton buildings much stronger they will be able to withstand all earthquakes, however, these extra strong structural elements will result in much higher stiffness of the building, which in turn will cause much higher base shear and absolute acceleration in the building floors, and consequently much more nonstructural damages, particularly to building's sensitive contents, such as equipment.

• In few cases the mushroom buildings have not been able to tolerate the earthquakes, which has been due to resonance. However, by a little strengthening of some structural elements, this building will be able to withstand all of the applied earthquakes. Of course, these will result in some more weight increase of these building comparing to the strong-skeleton ones.

Regarding that cost of a building's skeleton is around 30% of the total cost of whole building, the cost of the extra weight of the mushroom buildings in comparison to the strong-skeleton ones will be less than 10% in the total cost of the building. Although, it should be noted that the above percentages are rough, due to the limited number of buildings considered in the study. By this extra cost the building will remain basically intact and its damaged fuses will be easily repaired or replaced after the event. This is while the strong-skeleton buildings are not easily and quickly repairable, and the conventional buildings have to be demolished and rebuilt. Based on these facts, the use of mushroom structural system for low-rise building can be strongly recommended in seismic regions.

References

ASCE 41-13 (2013), Seismic Evaluation and Retrofit of Existing Building, American Society of Civil Engineering, USA.

ASCE 7-16 (2016), Minimum Design Loads and Associated Criteria for Buildings and Other Structures, American Society of Civil Engineering, USA.

Azuhata, T., Midorikawa, M., Ishihara, T. and Wada, A. (2002), "Shaking table tests on seismic response reduction effects of rocking building structural systems", *NIST Spec. Publ.*, 325-332.

Eatherton, M.R. and Hajjar, J.F. (2014), "Hybrid simulation testing of a self-centering rocking steel braced frame system", *Earthq. Eng. Struct. Dyn.*, **43**(11), 1725-1742.

FEMA P695 (2009), Quantification of Building Seismic Performance Factors, Federal Emergency Management Agency, USA.

Hosseini, M. and Alavi, S. (2014), "A kind of repairable steel buildings for seismic regions based on buildings' rocking motion and energy dissipation at base level", *J. Civil Struct. Eng.*, **1**(3), 157-163.

Hosseini, M. and Alyasin, S. (1996), "Deliberate directing of damage in lifeline systems subjected to earthquakes", *Proceedings of the Hazard-96 Symposium*, Toronto, Canada.

Hosseini, M. and Bozorgzadeh, S. (2013), "An innovative design for repairable regular steel buildings by using a 4-cell configuration structure with some inclined columns at base level, equipped with double-adas devices, and security cables at corners", *Proceedings of the Thirteenth East Asia-Pacific Conference on Structural Engineering and Construction*, Sapporo University, Hokkaido University Collection of Scholarly and Academic Papers.

Hosseini, M. and Ebrahimi, H. (2015), "Proposing a yielding-plate energy dissipating connection for circumferential columns of steel rocking buildings and investigating its circumferential properties by nonlinear proper finite element analyses", *Proceedings of the 6th International Conference on Advances in Experimental Structural Engineering*, University of Illinois, Urbana-Champaign, USA.

Hosseini, M. and Farsangi, E.N. (2012), "Telescopic columns as a new base isolation system for vibration control of high-rise buildings", *Earthq. Struct.*, **3**(6), 853-867.

Hosseini, M., Fekri, M. and Yekrangnia, M. (2016), "Seismic performance of an innovative structural system having seesaw motion and columns equipped with friction dampers at base level", *Struct. Des. Tall Spec. Build.*, **25**(16), 842-865.

Hosseini, M., Tirabadi, Y.M. and Hosseinzadeh, N.A. (2016), "An innovative seismic design for repairable regular steel buildings by using rocking motion and circumferential energy dissipating columns at base level", *Proceedings of the Thirteenth East Asia-Pacific Conference on Structural Engineering and Construction*, The Thirteenth East Asia-Pacific Conference on Structural Engineering and Construction (EASEC-13).

Kafaeikivi, M., Roke, D.A. and Huang, Q. (2016), "Seismic performance assessment of self-centering dual systems with different configurations", *Struct.*, **5**, 88-100.

Kam, W.Y., Pampanin, S. and Elwood, K. (2011), "Seismic performance of reinforced concrete buildings in the 22 February Christchurch (Lyttleton) earthquake", *Bull. N.Z. Soc. Earthq. Eng.*, **44**(4).

Kelly, J.M., Skinner, R.I. and Heine, A.J. (1972), "Mechanisms of energy absorption in special devices for use in earthquake resistant structures", *Bull. N.Z. Soc. Earthq. Eng.*, **5**(3), 63-88.

Khalkhali, S.M.H., Hosseini, M. and Aziminejad, A. (2017), "Dividing building's structure into 4 interactive rocking parts to make it repairable after major earthquakes", *Proceedings of the 16th World Conference on Earthquake Engineering*, Santiago, Chile, January.

Khanmohammadi, M. and Heydari, S. (2015), "Seismic behavior improvement of reinforced concrete shear wall buildings using multiple rocking systems", *Eng. Struct.*, **100**, 577-589.

Ma, Q.T., Wight, G.D., Butterworth, J.W. and Ingham, J.M. (2005), "Predicting the in-plane rocking behaviour of post-tensioned concrete walls subjected to earthquake excitations", *In the New Zealand Concrete Industries Conference.*

Mahdavi, V. (2018), "Proposing a method for creation of rocking motion in steel building with large plans and low heights for improving their seismic performance based on directed-damage design idea", Ph.D. Dissertation, Civil Engineering Department, Isfahan (Khorasgan) Branch, Islamic Azad University, Isfahan, Iran.

Midorikawa, M., Azuhata, T., Ishihara, T. and Wada, A. (2006), "Shaking table tests on seismic response of steel braced frames with column uplift", *Earthq. Eng. Struct. Dyn.*, **35**(14), 1767-1785.

Nakahara, K. and Nagase, T. (2000), "Earthquake response of rocking column in Japanese traditional wooden structure", *Summaries of Technical Papers of Annual Meeting Architectural Institute of Japan*.

Nejati, F., Hosseini, M. and Mahmoudzadeh, A. (2017), "Design of repairable regular steel buildings with square plan based on seesaw motion of building structure and using DADAS dampers", *Int. J. Struct. Integrity*, **8**(3), 326-340.

Nicknam, A. and Filiatrault, A. (2015), "Direct displacement-based seismic design of propped rocking walls", *Earthq. Spectra*, **31**(1), 179-196.

Nielsen, G.M., Almufti, I. and Mahin, S.A. (2010), "Performance of rocking core walls in tall buildings under severe seismic motions [C]", *Proceedings of the 9th US National and 10th Canadian Conference on Earthquake Engineering*, Toronto.

Otani, S., Hiraishi, H., Midorikawa, M. and Teshigawara, M. (2000), "Research and development of smart structural systems", *Proceedings of 12th World Conference on Earthquake Engineering*, Auckland, New Zealand.

Pollino, M. (2015), "Seismic design for enhanced building performance using rocking steel braced frames", *Eng. Struct.*, **83**, 129-139.

Priestley, M.J.N., Evison, R.J. and Carr, A.J. (1978), "Seismic response of structures free to rock on their foundations", *Bull. NZ Nat. Soc. Earthq. Eng.*, **11**(3), 141-150.

Qu, B., Sanchez-Zamora, F. and Pollino, M. (2014), "Mitigation of inter-story drift concentration in multi-story steel concentrically braced frames through implementation of rocking cores", *Eng. Struct.*, **70**, 208-217.

Seismic Design Code of Buildings (2014), *Standard No. 2800*, Building and Housing Research Center (BHRC), 4th Edition, Iran.

KT

Appendix: Final member sizes

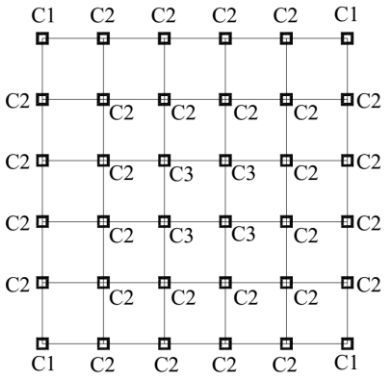

Type of Element	Number of Story		
	1	2	3
C1 Type Column	BOX 15×1.2	BOX 15×1.2	BOX 15×1.2
C2 Type Column	BOX 18×1.5	BOX 15×1.2	BOX 15×1.2
C3 Type Column	BOX 18×1.5	BOX 18×1.2	BOX 15×1
Brace	BOX 15×1.2	BOX 12×1	BOX 12×1
Beam	IPE 240	IPE 240	IPE 240

Type of Element	Number of Story			
	1	2	3	4
C1 Type Column	BOX 18×1.5	BOX 15×1.2	BOX 15×1.2	BOX 15×1.2
C2 Type Column	BOX 25×1.6	BOX 20×1.5	BOX 18×1.5	BOX 15×1.2
C3 Type Column	BOX 25×1.6	BOX 20×1.5	BOX 18×1.5	BOX 15×1.2
Brace	BOX 15×1	BOX 15×1	BOX 12×1	BOX 15×1.2
Beam	IPE 240	IPE 240	IPE 240	IPE 240

Type of Element	Number of Story				
	1	2	3	4	5
C1 Type Column	BOX 18×1.5	BOX 18×1.5	BOX 15×1.2	BOX 15×1.2	BOX 15×1.2
C2 Type Column	BOX 30×2	BOX 25×1.6	BOX 20×1.5	BOX 18×1.5	BOX 15×1.2
C3 Type Column	BOX 30×2	BOX 25×1.6	BOX 20×1.5	BOX 18×1.5	BOX 15×1.2
Brace	BOX 18×1.2	BOX 15×1	BOX 15×1	BOX 12×1	BOX 12×1
Beam	IPE 240	IPE 240	IPE 240	IPE 240	IPE 240

Type of Element	Number of Story					
	1	2	3	4	5	6
C1 Type Column	BOX 30×2	BOX 30×2	BOX 18×1.5	BOX 15×1.2	BOX 15×1.2	BOX 15×1.2
C2 Type Column	BOX 30×2	BOX 30×2	BOX 25×1.6	BOX 20×1.5	BOX 18×1.5	BOX 15×1.2
C3 Type Column	BOX 30×2	BOX 30×2	BOX 25×1.6	BOX 20×1.5	BOX 18×1.5	BOX 15×1.2
Brace	BOX 18×1.5	BOX 18×1.5	BOX 18×1.5	BOX 15×1.2	BOX 15×1.2	BOX 15×1.2
Beam	IPE 240	IPE 240	IPE 240	IPE 240	IPE 240	IPE 240

Type of Element	Number of Story						
	1	2	3	4	5	6	7
C1 Type	BOX	BOX	BOX	BOX	BOX	BOX	BOX
Column	30×2	30×2	18×1.5	15×1.2	15×1.2	15×1.2	15×1.2
C2 Type	BOX	BOX	BOX	BOX	BOX	BOX	BOX
Column	35×2	30×2	25×1.6	20×1.5	18×1.5	18×1.5	15×1.2
C3 Type	BOX	BOX	BOX	BOX	BOX	BOX	BOX
Column	30×2	30×2	30×2	25×1.6	20×1.5	18×1.5	15×1.2
Brace	BOX 18×1.5	BOX 18×1.5	BOX 18×1.5	BOX 18×1.5	BOX 18×1.5	BOX 18×1.5	BOX 18×1.5
Beam	IPE 240	IPE 240	IPE 240	IPE 240	IPE 240	IPE 240	IPE 240